Limnol. Oceanogr., 49(6), 2004, 2242–2255

Methane along the western Mexican margin

Francis J. Sansone[1] *and Andrew W. Graham*[2]
University of Hawaii, Department of Oceanography, 1000 Pope Road, Honolulu, Hawaii 96822

William M. Berelson
University of Southern California, Department of Earth Sciences, 3651 Trousdale, Los Angeles, California 90089

Abstract

We investigated the processes controlling the water-column and sediment methane distributions at 14 stations along the western Mexican margin, in and around the Gulf of California. Stations were grouped into two categories: coastal basins and open margins. Diffusive methane fluxes from the sediment at all sites, as estimated from sediment methane gradients, were 0.24–5.5 μmol m^{-2} d^{-1}, with the highest fluxes observed on the Pacific margin of Baja California at both basin and open-margin sites. These high rates occur despite the lack of significant terrestrial input to these sediments, reflecting the importance of upwelling-induced productivity. Methane concentrations in the upper water column were supersaturated with respect to the present atmosphere at all sites, with sea–air fluxes of methane of 0.5–5.9 μmol m^{-2} d^{-1}. Four of the open-margin sites had seafloor depths extending below the oxygen minimum zone (~400–800 m) and contained low methane concentrations below the subsurface methane maximum. The remaining margin site was shallow (593 m), with a seafloor that intersected the oxygen minimum zone, and had elevated methane concentrations throughout the water column; this indicates that such sediments may be a significant source of methane to the eastern tropical North Pacific (ETNP). The seawater within silled basin sites also had supersaturated methane concentrations, reflecting the anoxic conditions within the basins. However, methane levels were low at the sill depth, indicating that the silled basins were unlikely to be significant sources of methane to the ETNP. We observed an inverse relationship between methane concentration and δ^{13}C-CH_4 value in the basin waters, consistent with biological aerobic oxidation of methane being released from the sediment; an apparent kinetic isotopic fractionation factor of 1.0100–0.0038 was calculated for this process. Isotopically heavy methane resulting from similar oxidation of seafloor-derived methane may be the source of large pools of heavy methane previously observed offshore in the ETNP.

Methane is a potent greenhouse gas and an important component of atmospheric chemical cycles. The concentration of methane in the atmosphere has more than doubled (700 ppb to >1,750 ppb) over the last 250 yr and is now increasing at a rate of ~2% per year (Cicerone and Oremland 1988; IPCC 2001; Steele et al. 2002), implying that in the near future, methane could have a larger role in global warming and atmospheric chemistry than it does today.

While the open ocean appears to be a relatively small source of methane to the atmosphere (e.g., Breas et al. 2001), methane cycling in the open ocean is not fully understood. Additionally, coastal areas and other marine environments rich in methane are significant sources to the atmosphere (e.g., Owens et al. 1991; Bange et al. 1994; Sansone et al. 1998*b*; Oudot et al. 2002). Understanding the natural sources and sinks of methane is vital to determining future changes in atmospheric methane concentrations.

[1] Corresponding author (sansone@hawaii.edu).
[2] Present address: Polaris Applied Sciences, Inc., 12509 130th Lane NE, Kirkland, Washington 98034.

Acknowledgments

We thank Lowell Stott and the rest of the science party of the CALMEX cruise; the officers and crew of the RV *New Horizon*; Brian Popp and Terri Rust for assistance with the methane stable-carbon isotopic ratio measurements; and Dave Valentine and an anonymous reviewer for very helpful comments. This research was supported by the U.S. National Science Foundation, grants OCE-9911649 and OCE-0002250. SOEST contribution no. 6437.

Water-column methane profiles for the open ocean have been well documented (Lamontagne et al. 1973; Scranton and Brewer 1977; Conrad and Seiler 1988; Holmes et al. 2000). One common feature of these profiles is subsurface methane maxima in the upper 300 m, often associated with the pycnocline. Subsurface methane maximum concentrations range between 2.0 and 4.0 nmol L^{-1} and are 30–70% supersaturated with respect to the atmosphere (e.g., Lamontagne et al. 1973; Burke et al. 1983; Holmes et al. 2000). While in some areas this maximum may be the result of horizontal advection from methane-rich source regions (Scranton and Farrington 1977; Brooks 1979; Sansone et al. 1999) or from coastal upwelling (Rehder et al. 2002), the majority of researchers have attributed this supersaturation to in situ methane production (e.g., Scranton and Brewer 1977; Conrad and Seiler 1988; Holmes et al. 2000). Supersaturation of methane in deep ocean waters can occur as a result of hydrothermal discharge (e.g., de Angelis et al. 1993; Mottl et al. 1995; Cowen et al. 2002), release of methane-rich pore waters (e.g., Reeburgh 1976; Scranton and Farrington 1977), or seepage from hydrates (Suess et al. 1999) or other gas reserves (Brooks 1979).

Typical dissolved methane profiles in marine sediments are concave upward (e.g., Martens and Berner 1974; Reeburgh 1976; Reeburgh and Heggie 1977), with low concentrations (<0.05 mmol L^{-1}) extending from the sediment–water interface to sediment depths between 20 cm (Martens and Berner 1974) and 1 m (Iversen and Jorgensen 1985). These low methane concentrations correspond to the active

sulfate reduction zone in which sulfate concentrations are at least 10% that of seawater sulfate (Martens and Berner 1977). Sulfate becomes depleted below this zone and methane concentrations increase dramatically, reaching 5–15 mmol L^{-1} (Reeburgh and Heggie 1977).

Methanogenesis and sulfate reduction are generally considered to be mutually exclusive (Barnes and Goldberg 1976; Oremland and Taylor 1978; Warford et al. 1979). It appears that sulfate-reducing bacteria may successfully outcompete methanogens for hydrogen in the presence of sulfate, favoring limited production of methane by ''noncompetitive'' substrates in the sulfate reducing zone. However, once the sulfate has been depleted, carbon dioxide reduction and possibly acetate fermentation become the primary sources of methane (Whiticar 1996). Sulfate-reducing bacteria are also able to oxidize methane in anaerobic environments (e.g., Martens and Berner 1977; Valentine and Reeburgh 2000). This process is effective in limiting the flux of methane from anoxic settings where dissolved sulfate is present, such as marine sediments with oxic–suboxic surface layers.

Stable carbon isotopic ratios—Stable carbon isotopic ratios of methane (δ^{13}C-CH_4) have been used to determine methane production and consumption processes in a variety of environments, such as coastal sediments (Martens et al. 1986), hydrothermal plumes (Welhan 1988), biogenic gas fields (Schoell 1980), and the oceanic water column (Sansone et al. 1997, 1999). Biogenic methane formation fractionates the carbon isotopes of the substrate, leaving the substrate enriched in ^{13}C and the newly formed methane depleted in ^{13}C. δ^{13}C values of biogenic methane can range from -110 to -50‰ (Whiticar et al. 1986; Whiticar 1996). Inorganic methane production has different fractionation effects and usually occurs at higher temperatures than biogenic methane production, resulting in δ^{13}C values of -50 to -20‰ (Whiticar et al. 1986; Whiticar 1996). Microbial oxidation of methane preferentially utilizes $^{12}CH_4$, resulting in the ^{13}C enrichment of the residual methane (e.g., Coleman and Risatti 1981). Additionally, the isotopic ratio of the methanogenic substrates (Martens et al. 1986; Whiticar 1986) and mixing of methane with different δ^{13}C values (Sansone et al. 1999) exert influence on δ^{13}C values.

Eastern tropical North Pacific/Mexican margin—The eastern tropical North Pacific (ETNP) is an area of high surface productivity derived from coastal upwelling (e.g., Deuser 1975). Severely depleted seawater oxygen concentrations (<1 μmol L^{-1}) result from the decomposition of organic matter as it settles through the water column. The low oxygen core extends >1,500 km off the coast of Mexico (Fig. 1) and provides an ideal environment for studying suboxic/anoxic marine chemistry (Cline and Richards 1972; Sansone et al. 2001). Methane has been investigated in the region on two previous occasions, by Burke et al. (1983) and Sansone et al. (2001).

Burke et al. (1983) occupied nine stations in the ETNP on a cruise track roughly parallel to the Mexican coastline (Fig. 1). As expected, subsurface methane concentrations were supersaturated with respect to the atmosphere, with concentrations of ca. 2.0–6.5 nmol L^{-1} (44–145 nl L^{-1}) be-

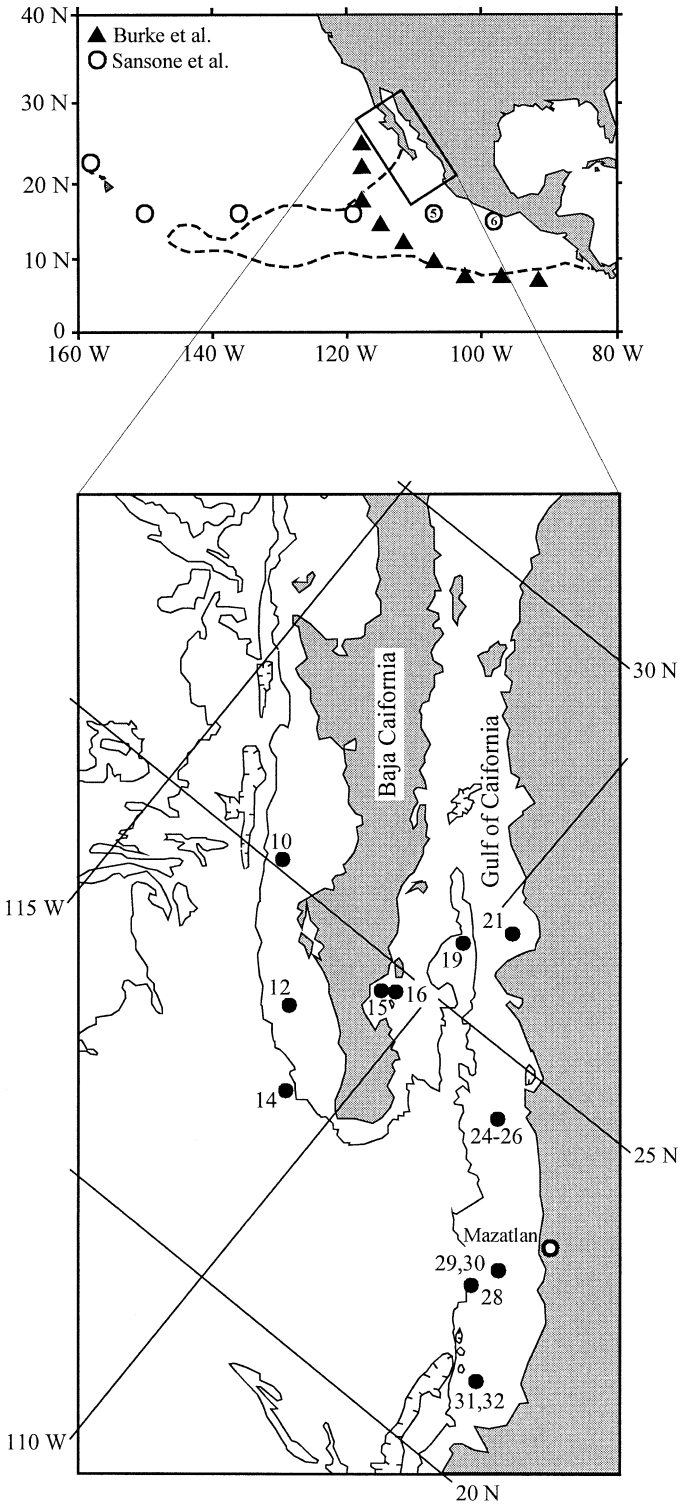

Fig. 1. The eastern tropical North Pacific, with stations of Burke et al. (1983) and Sansone et al. (2001) shown (upper map); CALMEX hydrocast and sediment-core stations (lower map). Stations 5 and 6 of Sansone et al. are labeled. Dashed line in the upper map represents the 9 μmol L^{-1} dissolved oxygen isopleth at 400 m in depth (data from http://ferret.wrc.noaa.gov/Ferret/LAS/ferret_LAS.html). The depth contour interval of the lower map is 1,000 m.

Table 1. Physical characteristics of the CALMEX stations, grouped into basin and open-margin sites.

	Hydrocast station	Core station	Name	Water depth (m)	Sill depth (m)	Comments
Basin	10	10	Soledad	541	290	
	15	15	Alfonso	410	325	Collects terrigenous sediment
	16	—	Lobos	387	—	Unsilled basin offshore of Sta. 15
	32	31	San Blas	450	50	Very shallow sill
Open-margin	—	12		713	—	Close to Station 14
	14	—	Magdelena	1,458	—	Deep; high O_2 at bottom
	19	—	Carmen	993	—	
	—	21	Carmen	575	—	
	24	—	Pescadero	1,035	—	
	—	26	Pescadero	600	—	
	28	—	Mazatlan	2,116	—	Deep; near-bottom waters not sampled
	30	—	Mazatlan	593	—	
	—	29	Mazatlan	422	—	

tween 50-m and 150-m depths. At stations in the core of the oxygen-depleted zone, this supersaturation extended down to at least 407 m (maximum depth reported). In an attempt to determine the source of this methane, Burke et al. (1983) also measured total suspended matter (TSM), particulate organic carbon (POC), chlorophyll *a,* and adenosine triphosphate (ATP). While at some stations correlations arose between methane and either TSM, chlorophyll *a,* or ATP, these correlations were limited to individual stations and were not present at all the stations sampled. To explain the excess methane concentrations in the ETNP, Burke et al. concluded that in situ production in reducing microenvironments, associated with suspended particles or phyto- and zooplankton, was the most logical methane source. The possibility of advection from coastal waters and/or sediments was rejected as a result of the belief that the shelf could only influence a narrow portion of the ETNP and could not support the elevated concentrations observed at all stations in the upper 200 m of the water column.

Sansone et al. (2001) sampled at six stations, starting in the oligotrophic North Pacific gyre, north of Hawaii, and extending across the ETNP to the coastal upwelling zone, 110 km off the coast of Mexico (Fig. 1). Highly elevated methane concentrations were measured at Sta. 5 and 6, the two stations closest to the Mexican shelf. Maximum concentrations at Sta. 6 were 28 nmol L^{-1} at 350 m in depth, with concentrations over 10 nmol L^{-1} between 250 and 650 m in depth. Methane concentrations at these depths remained above 10 nmol L^{-1} beyond Sta. 5, more than 1,000 km from the coast of Mexico.

The upper section of the large pool of methane at Sta. 5 and 6 (200–350 m in depth) contained methane with an isotopic composition of −45 to −42‰ (Sansone et al. 2001). The lower part of the pool (350–600 m), however, was isotopically enriched, with $\delta^{13}C\text{-}CH_4$ values of −30 to −26‰ at Sta. 6 and higher values (−20‰) at Sta. 5. These isotopic data led Sansone et al. to the conclusion that in situ methane production was occurring in the upper half of the methane pool, leading to the observed isotopically depleted ratios. The lower half of the pool, however, was hypothesized to have been advected out to the ETNP, and microbial oxidation during this advection was the cause of the isotope enrichment. The source of the lower half of the pool was assumed to be the organic-rich sediments and/or anoxic waters (Hartnett et al. 1998) of the western Mexican margin.

CALMEX cruise—In the period extending from November to December of 2001, the CALMEX (California–Mexico) expedition conducted sediment coring and hydrocasts at 14 stations near the entrance to the Gulf of California (Fig. 1). This cruise provided an opportunity to measure methane concentrations and methane stable-carbon isotopic ratios in the water column and sediments at several sites along the margin. Since no studies of this kind have been reported for this region of the ETNP, these data provided a first look into methane and methane cycling processes along the western Mexican margin. The results of this investigation also helped clarify the source of the large pool of dissolved methane present in the ETNP.

Methods

Sample locations—Samples were collected at 10 sites in the Gulf of California/ETNP region, with water depths ranging from 375 to 1,445 m; hydrocasts were conducted at nine of these sites, and sediment cores were recovered from seven of them. Station locations are shown in Fig. 1, and Table 1 lists the water depths, the sill depths (where applicable), and general information for each station.

Sample collection—Water samples for methane concentrations and isotopic ratios were collected with twelve 12-liter Niskin bottles attached to a rosette. Seawater was transferred from the Niskin bottles into 230-ml glass serum bottles via Tygon tubing. Sample bottles were flushed with at least 500 ml of seawater before slowly removing the Tygon tubing. The samples were visually inspected for air bubbles and poisoned with 0.25 ml of saturated mercuric chloride solution. Gray butyl rubber stoppers and aluminum crimp seals were used to seal the bottles, which were then stored in boxes until they could be analyzed on shore.

Both multicoring and gravity coring techniques were used

to obtain sediment pore-water samples. Multicoring consisted of collecting cores with eight separate, removable barrels attached to a frame lowered from the ship. Multicores were used to sample the sediment–water transition and up to 60 cm of sediment below this interface. Gravity coring used polyvinyl chloride tubes weighted on one end and lowered rapidly into the sediment. Gravity coring yielded cores up to 5 m long. Multicores and gravity cores were both collected at Sta. 10, 12, 15, 21, 26, and 29, but only a multicore was recovered at Sta. 31.

When the multicore array was recovered, a single multicore was placed in an argon-filled glove bag and sampled for pore-water methane concentrations and methane isotopic ratios. The core was extruded out of the top of the barrel, and subsamples of the core were taken by inserting a tipless, 3-ml plastic syringe horizontally into the core. A butyl rubber stopper was inserted into the end of the syringe, once it was removed from the core, to keep the subsample isolated from the surrounding air until all samples were taken (Pope et al. 1995). Each subsample was transferred to a preweighed 20-ml glass serum vial that had been flushed with helium gas for at least 1 min prior to receiving the sample. A helium-sparged solution, containing 1 ml saturated mercuric chloride and 2.5 ml deionized water, was added to each vial before the latter was capped with a gray butyl rubber stopper and crimp-sealed with an aluminum cap. The samples were then homogenized by vortex shaking for at least 1 min and stored in boxes until analyzed on shore. Spacing between samples within a multicore was ~5.5 cm.

Gravity cores were cut into sections ranging between 40 and 60 cm, and these sections were then placed in a 150-liter plastic bucket that was overflowing with argon gas introduced at the bottom of the bucket. Syringes were then inserted vertically into the top of the core sections and subsamples were removed. Butyl rubber stoppers were inserted into the ends of the syringes, and the subsamples were treated in a similar manner to those of the multicores. Samples from the gravity cores were usually taken from one end of the sections, and, thus, the spacing between these samples ranged between 40 and 60 cm.

Chemical analyses—Water-column methane concentrations were determined with a Hewlett-Packard 5890 gas chromatograph, following the purge-and-trap technique described by Brooks et al. (1981). Methane gas was separated with a 2 × 3–mm stainless-steel analytical column packed with Porapak QS and measured with a flame ionization detector. The gas chromatograph was calibrated by repeated analyses of a 45.2-ppm CH_4 standard (in nitrogen) before, during, and after a series of sample analyses, using the cold-trapping technique used for samples. Analytical precision using this standard was better than −1% (1 standard deviation [SD]), and drift during analysis was <2%. The combined precision of the analysis and sample collection was determined by Gharib (2000) to be 8%.

Methane isotopic ratios were determined at the University of Hawaii using an isotope–ratio-monitoring gas chromatography/mass spectrometry procedure (Popp et al. 1995; Sansone et al. 1997). Methane was separated on a 25 × 0.32–mm PoraPLOT-Q analytical capillary column at −25°C. The methane was then converted to CO_2 using NiO_2/Pt at 1,150°C, and the isotopic composition determined with a Finnigan MAT 252 mass spectrometer. The analytical precision was ±0.8‰ when analyzing seawater samples with dissolved methane concentrations of >1.5 nmol L^{-1} (Sansone et al. 1997). These results are reported using the standard $\delta^{13}C$ convention:

$$\delta^{13}C = 1{,}000[(({}^{13}C/{}^{12}C)_{sample}/({}^{13}C/{}^{12}C)_{standard}) - 1] \quad (1)$$

Results are relative to the Pee Dee Belemnite carbon standard (Craig 1957).

Sediment pore-water methane concentrations were determined by analysis of the sample-vial headspace, using the same gas chromatograph as above. Analytical and sampling precision, determined by repeated analysis of single samples and analysis of duplicate samples from the same depth, was 2%.

Sulfate concentrations were determined gravimetrically by the addition of 1 mol L^{-1} barium chloride solution and subsequent precipitation of barium sulfate, using 1.8 ml of pore water. This precipitate was then filtered on 0.8-μm Nuclepore polycarbonate filters and weighed. However, replicate seawater analyses were on average 5% higher than 28 mmol L^{-1}, the expected concentration of seawater; thus, all sample sulfate concentrations were decreased by 5%. Analytical precision was (0.84 mmol L^{-1} [1 SD]), based on replicate analyses of seawater.

Water-column dissolved oxygen concentrations were determined using an MI-730 oxygen electrode (Microelectrodes) designed for use with a voltmeter. The voltage readings were converted to oxygen concentrations by assuming that the surface waters were in equilibrium with the atmosphere at the measured temperature and salinity. The voltage reading at the surface was then set equal to this calculated oxygen concentration, and the voltage readings throughout the water column were then scaled to the surface water reading. No measurement was made of the precision of the electrode. Samples collected in the core of the oxygen minimum zone had measured dissolved oxygen concentrations of <1 mmol L^{-1}, but the method was not sufficiently accurate to determine if dissolved oxygen was in fact absent at these depths.

Pressure, density, and light transmission data were acquired with a Seabird 911 conductivity-temperature-depth (CTD) attached to the rosette. Sediment porosity was calculated by weighing a known volume of wet sediment and then drying it in an oven to remove all water; a salt correction (accounting for the mass of salt in the pore water) was applied assuming a salinity of 34. The difference in weight before and after drying was assumed to be the weight of the water in the sediment, which was then converted to a water volume. The water volume was divided by the volume of wet sediment to derive the porosity value.

Calculations—Methane solubility: Air-equilibrated methane solubility was calculated (Yamamoto et al. 1976) using the temperature and salinity of each individual sample and assuming an atmospheric methane mixing ratio of 1,775 ppbv, the atmospheric methane mixing ratio at Mauna Loa during the period between November and December 2001

(Steele et al. 2002). The latter was assumed to be the mixing ratio at our sampling sites during the CALMEX cruise because of the similar latitudes of Mauna Loa and the CALMEX sampling sites.

Air–sea methane flux: The flux of methane from seawater to the atmosphere at each station was calculated using the following model (Barber et al. 1988):

$$F = K_L(C_m - C_{eq}) \quad (2)$$

where F is the flux of methane out of the water (μmol m^{-2} d^{-1}), K_L is the gas transfer coefficient (m d^{-1}), C_m is the measured methane concentration of the surface water (μmol m^{-3}), and C_{eq} is the calculated methane concentration in equilibrium with the atmosphere (μmol m^{-3}), as detailed above. K_L values were estimated using the empirical wind speed/K_L relationship given by Barber et al. (1988), corrected for the in situ water temperature. The daily mean wind speed for each station was obtained from QuikSCAT satellite scatterometer data (http://www.ifremer.fr/cersat/facilities/browse/mwf/qscat_day.htm). An atmospheric methane mixing ratio of 1,775 ppbv (Steele et al. 2002) was again assumed.

Sediment–seawater methane fluxes: Apparent diffusive sediment–seawater methane fluxes were calculated using Fick's first law of diffusion, modified for sediments (Berner 1971; Martens and Klump 1980):

$$J_{sed} = -\phi D_s(\partial C/\partial z)_{pw} \quad (4)$$

where J_{sed} is the flux out of the sediment (μmol cm^{-2} s^{-1}), ϕ is the porosity (cm^3_{pw} cm^{-3}_{sed}, where pw denotes pore water), D_s is the bulk sediment diffusivity (cm^2_{sed} s^{-1}), and $(\partial C/\partial z)_{pw}$ is the methane concentration gradient at the sediment–water interface. $(\partial C/\partial z)_{pw}$ was estimated by fitting a regression line to the concentration data from the upper 30 cm at all stations except Sta. 12, where the concentrations in the upper 25 cm were used. The error associated with the $(\partial C/\partial z)_{pw}$ calculation and the resulting methane flux, due to error in the methane concentration measurements, was ~10%. D_s was calculated from the following equation (McDuff and Gieskes 1976):

$$D_s = DF^{-1}\phi^{-1} \quad (5)$$

where D is the free solution diffusivity (cm^2_{pw} s^{-1}) and F is the ''resistivity ratio'' (cm_s cm^{-1}_{pw}). Temperature-corrected D values were extrapolated from data by Sahores and Witherspoon (1970). A value of 1.3 was used for F, taken from similar work done by Martens and Klump (1980) in fine-grained sediments.

Isotopic fractionation factor: The apparent biological kinetic isotopic fractionation factor (α) for microbial methane oxidation during the transport of methane through the water column (Coleman and Risatti 1981) was calculated as follows:

$$\alpha = \frac{\ln(C/C_o)}{\ln[(R + 1{,}000)/(R_o + 1{,}000)]} \quad (6)$$

where C_o and R_o are the initial methane concentration and isotopic ratio, respectively, and C and R are the residual concentration and isotopic ratio, respectively. If the residual methane is derived from microbial oxidation of the initial methane, the fractionation factor should be in the range of 1.0042 to 1.0250 (Coleman and Risatti 1981; Martens et al. 1999; Sansone et al. 1999, 2001; Grossman et al. 2002). Unfortunately, the accuracy of the dissolved oxygen measurements prevented a determination of whether the observed methane oxidation occurred under anoxic or merely suboxic conditions.

Results and discussion

Upper water column dynamics—Sea–air flux: All of the CALMEX stations were supersaturated with respect to the atmosphere (50–190%) in the upper 200 m, indicating that these stations are sources of methane to the atmosphere (Figs. 2, 3). Calculated sea–air methane fluxes for each sampling station are presented in Table 2, along with sampling dates and the corresponding sea–surface wind speeds. The sea–air fluxes from the CALMEX stations during sampling were 0.5–5.9 μmol m^{-2} d^{-1}, with the dominant control being wind speed rather than the surface methane concentration (Table 2). The elevated concentrations in the surface waters at the CALMEX sites might be expected to drive strong fluxes of methane into the atmosphere, as noted above for other sites; however, the low wind speeds typical of this region (3–6 m s^{-1}; http://www.ifremer.fr/cersat/facilities/browse/mwf/qscat_day.htm) generally prevent this, similar to the situation in the eastern equatorial Atlantic (Oudot et al. 2002).

Open-ocean regions with reported sea–air methane fluxes include the north Pacific subtropical gyre (1.4–1.7 μmol m^{-2} d^{-1}, Holmes et al. 2000), the eastern tropical north Pacific (2.3 μmol m^{-2} d^{-1}, Sansone et al. 2001), the equatorial Atlantic (1.2–2.0 μmol m^{-2} d^{-1}, Oudot et al. 2002), and the eastern south Pacific (−0.74–4.1 μmol m^{-2} d^{-1}, Kelley and Jeffrey 2002). Significantly elevated fluxes (>4 μmol m^{-2} d^{-1}) have been reported for coastal waters (e.g., Bange et al. 1994) and upwelling areas (Kelley and Jeffrey 2002) as a result of high surface–water methane concentrations. Thus, the calculated CALMEX fluxes are intermediate between those of open-ocean and coastal regions.

Subsurface maxima—Subsurface methane maxima were present between 75 and 100 m at all stations except for Sta. 30 and 32. (Note that there was often 50–100 m separating samples and it is unlikely that the true maxima have been sampled at each station.) Concentrations in these shallow maxima ranged between 4.6 and 10.1 nmol L^{-1} (92% and 340% supersaturated with respect to the present atmosphere). These features may be produced in situ in anoxic subenvironments, including suspended particles, fecal pellets, zooplankton, and fish guts (Scranton and Brewer 1977; Oremland 1979; de Angelis and Lee 1994; Karl and Tilbrook 1994). Another possibility is that the subsurface methane maxima are a result of methane-rich water advecting from sediments, rivers, or estuaries closer to shore (Scranton and Farrington 1977; de Angelis and Lilley 1987; Sansone et al. 1999). It is likely that a combination of these processes occur at the CALMEX stations.

The only δ^{13}C-CH_4 values of subsurface local maxima in this study, measured at Sta. 10 and 15, were −41.6‰ and

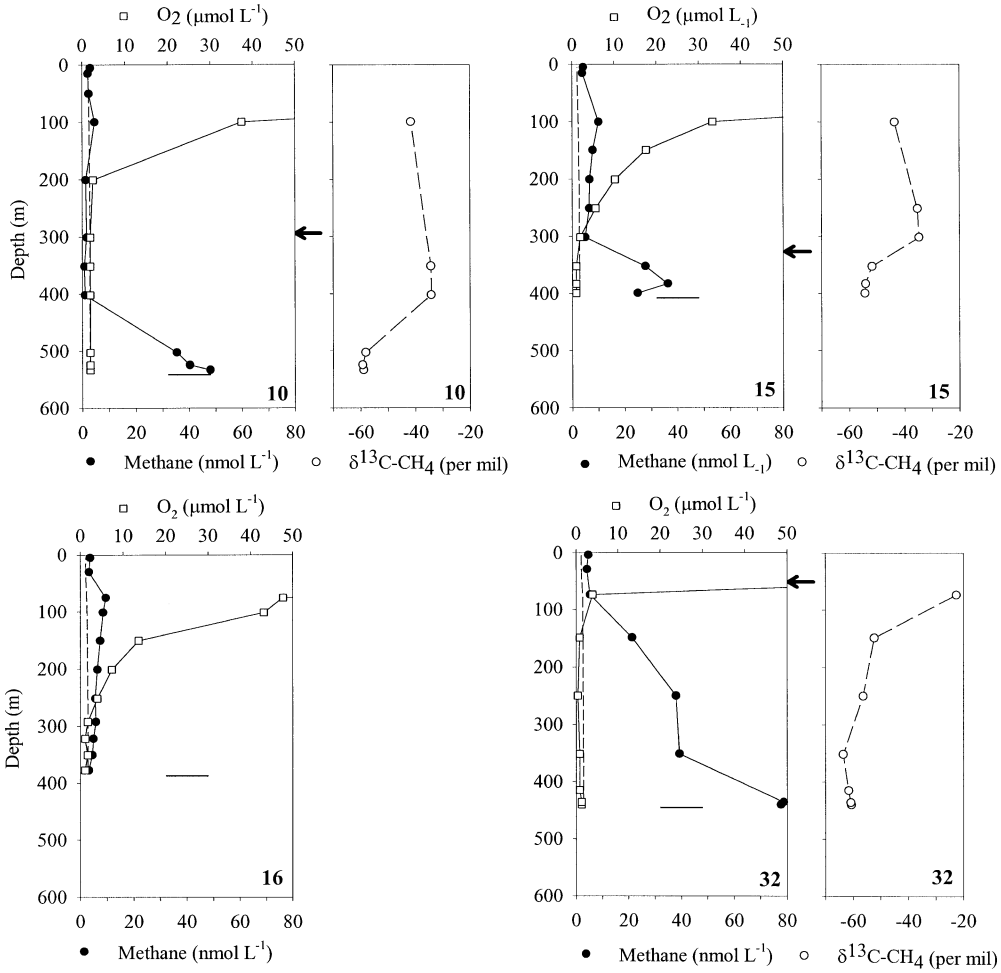

Fig. 2. Methane concentration, dissolved oxygen concentration, and methane stable-carbon isotopic ratio profiles for basin stations. Station numbers are in the lower right-hand corner of each panel. Arrows indicate the sill depths of silled basins. Dashed lines indicate the methane concentration in equilibrium with the present atmosphere at in situ conditions (*see* text for details). Horizontal bars indicate the seafloor depth.

−43.6‰, respectively. Although Sta. 10 and 15 are silled basin sites, this is unlikely to affect the upper water-column methane dynamics, since the elevated bottom-water methane concentrations at Sta. 10 and 15 decreased dramatically before reaching the sill depth (discussed later). These δ^{13}C values (−41.6 to −43.6‰) are heavier than would be expected because of methanogenesis (−50 to −110‰; Whiticar et al. 1986; Whiticar 1996), yet they are still within 2.5‰ of the δ^{13}C values (−44 to −47 ‰) reported by Holmes et al. (2000) for methane produced in situ in the subsurface maximum of the subtropical North Pacific. Incubations performed by Holmes et al. showed these isotopically enriched values can result from methanogenesis in anoxic subenvironments (particulate organic matter), where methane substrates may become limiting and/or methanogenesis proceeds utilizing methylated compounds. Alternatively, microbial oxidation of advecting methane from coastal environments would cause the δ^{13}C values to become elevated and could also explain the relatively heavy δ^{13}C values found at these two stations.

Lower water-column and sediment dynamics—Variations in the water-column methane level were observed below 200 m (Figs. 2, 3). The morphology of the seafloor present at each station (e.g., silled basin, open margin), the seafloor relationship to the oxygen minimum zone, the release of methane from the sediment, and advection of methane-rich waters likely have a larger influence than in situ methanogenesis in producing this variation.

Sediment pore-water sulfate concentrations were at seawater values near the sediment–water interface and then decreased monotonically with depth (Figs. 4, 5). The change in sulfate concentration over the upper 40 to 50 cm (the surface sulfate gradient) is shown in Table 3 for each station, along with the depths at which sulfate concentrations decrease to <3 mmol L^{-1}; the latter ranged from 80 cm at Sta. 10 to >400 cm at Sta. 21 and 29.

Methane remained low (0.3–30 μmol L^{-1}) until sulfate concentrations were depleted to $\sim$3 mmol L^{-1}, at which point methane concentrations increased dramatically. Concentrations of methane in the sulfate-depleted zone ranged

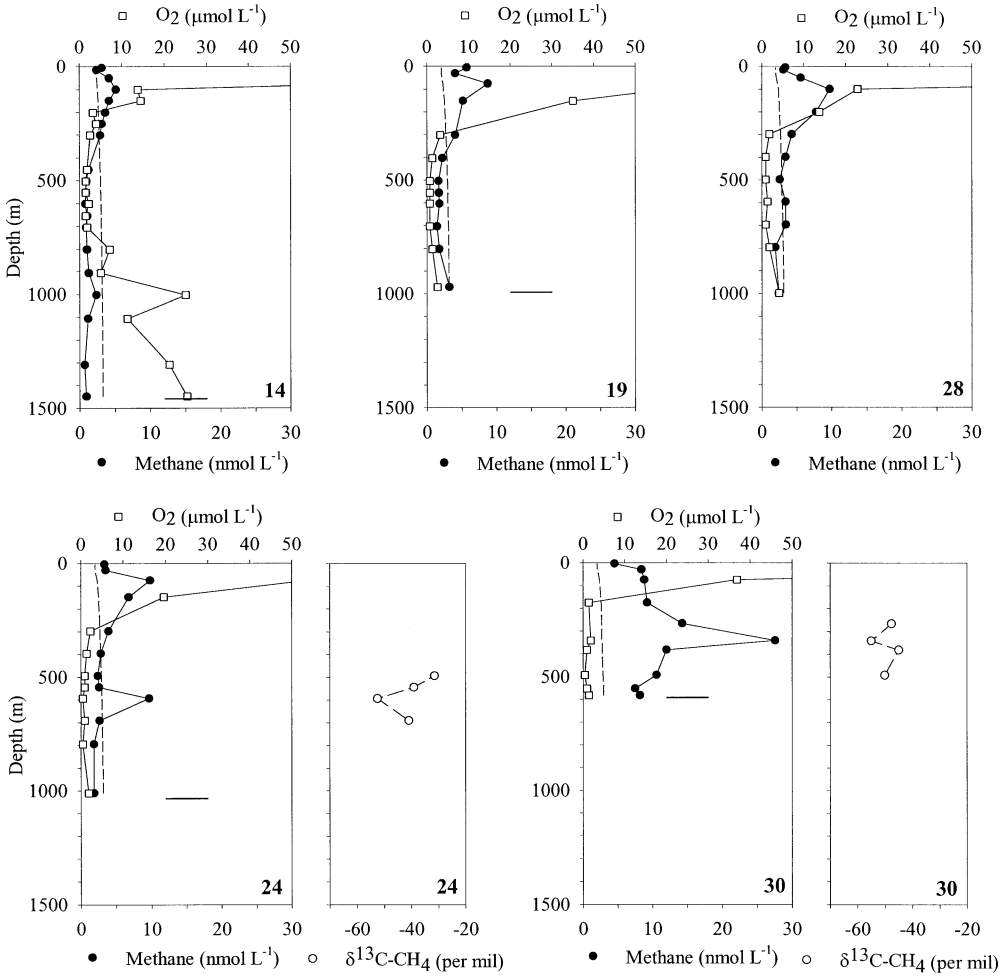

Fig. 3. Methane concentration, dissolved oxygen concentration, and methane stable-carbon isotopic ratio profiles for open-margin stations. Station numbers are in the lower right-hand corner of each panel. Dashed lines indicate the methane concentration in equilibrium with the present atmosphere at in situ conditions (*see* text for details). Horizontal bars indicate the seafloor depth.

from 0.14 to 6 mmol L^{-1}, with the maximum value observed at Sta. 12. Methane concentrations at Sta. 21 and 29 remained below 70 μmol L^{-1} as a result of deep sulfate-reducing zones. Sulfate concentrations at these stations were large enough to inhibit extensive methanogenesis and to keep methane concentrations low throughout the length of the core. Detailed methane profiles for the upper 50 cm at each site, used to calculate apparent diffusive methane fluxes, are presented in Figs. 4 and 5; the calculated fluxes are listed in Table 3.

Table 2. Calculated sea–air methane fluxes for CALMEX hydrocast stations, along with sampling dates and the corresponding sea–surface wind speeds. See text for details.

Station	Sampling date (2001)	Wind speed (m s^{-1})	Flux (μmol m^{-2} d^{-1})
10	24 Nov	8	3.5
14	25 Nov	5	1.1
15	28 Nov	11	5.9
16	28 Nov	11	5.9
19	29 Nov	7	2.7
24	1 Dec	7	2.7
28	3 Dec	7	2.7
30	4 Dec	4	0.5
32	4 Dec	3	0.5

Silled basins—Sta. 10 and 15—Three silled basins were sampled during the CALMEX cruise: (1) Sta. 10, with a water depth of 540 m and a sill depth of 290 m, is situated off the western coast of Baja California; (2) Sta. 15, with a water depth of 410 m and a sill depth of ~325 m, is situated off the eastern coast of Baja California inside La Paz Bay; the Sta. 15 basin acts as a trap for terrigenous sediments from alluvial fans feeding the bay (Nava-Sanchez et al. 2001); (3) Sta. 32 is distinctive because of its very shallow sill depth (<50 m); consequently, this station (along with the corresponding sediment core at Sta. 31) will be discussed in detail in the next section.

The high methane concentrations of the deep waters (25–78 nmol L^{-1}) differentiate the silled-basin sites from the open-margin stations. These stations have methane concen-

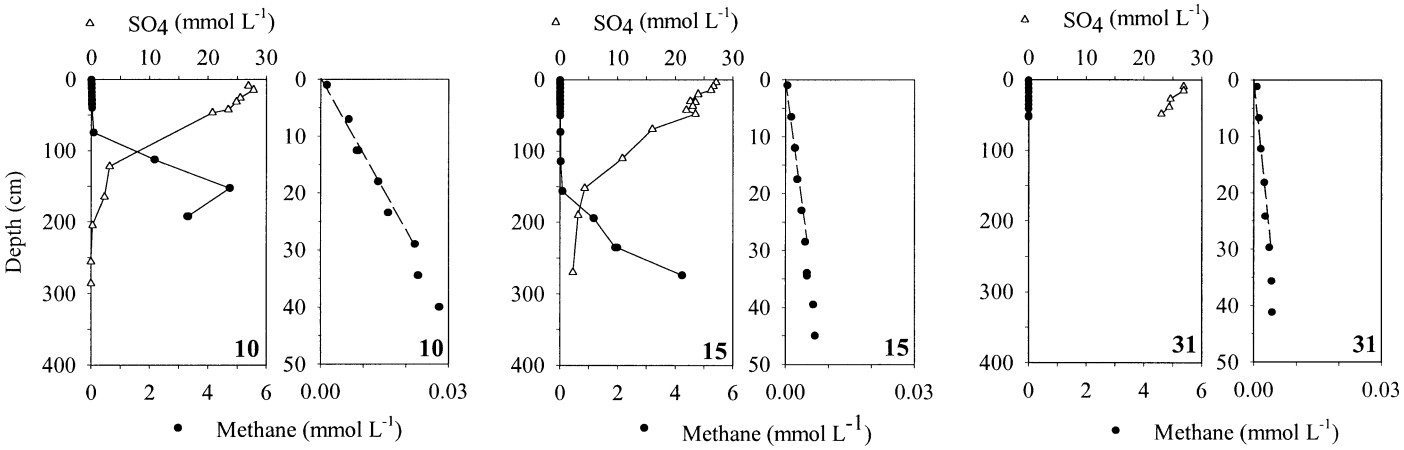

Fig. 4. Sediment methane and sulfate concentration profiles for basin stations (left-hand panels), along with detailed profiles of the methane concentration in the upper 50 cm (right-hand panels). Station numbers are in the lower right-hand corner of each panel. Linear regressions of the methane concentration gradients in the right-hand panels are for data from the upper 30 cm.

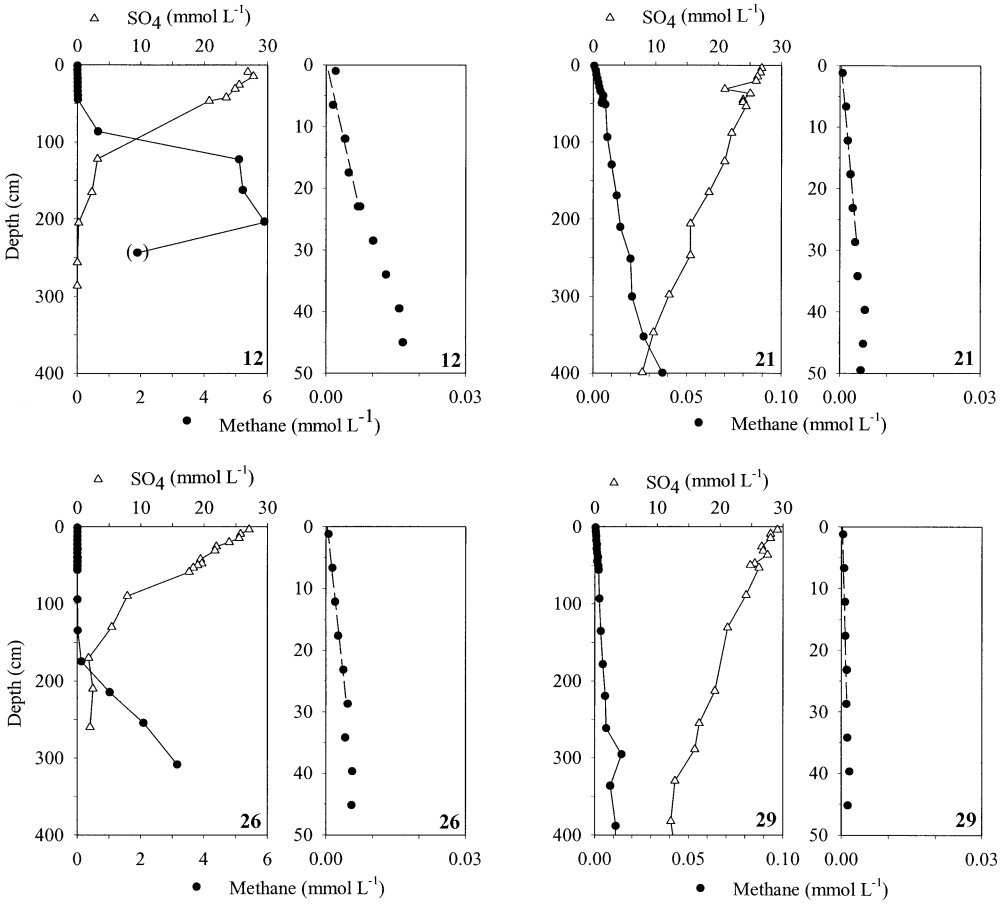

Fig. 5. Sediment methane and sulfate concentration profiles for open-margin stations (left-hand panels), along with detailed profiles of the methane concentration in the upper 50 cm (right-hand panels). Station numbers are in the lower right-hand corner of each panel. Linear regressions of the methane concentration gradients in the right-hand panels are for data from the upper 30 cm (25 cm at Sta. 12).

Table 3. Chemical characteristics of CALMEX sediment-coring stations. The methane flux standard error is 10% (see text); n.a., data not available. C : N ratio is from 0–4-cm sediment depth.

Station	Diffusive methane flux (μmol m^{-2} d^{-1})	Surface sulfate gradient (mmol L^{-1} cm^{-1})	Depth to sulfate depletion (cm)	C : N ratio at surface
10	5.5	0.24	80	4.01
12	1.7	0.20	100	5.92
15	1.1	0.14	170	8.98
21	0.63	0.06	>400	9.29
26	0.87	0.17	180	11.01
29	0.24	0.06	>400	3.12
31	0.71	0.10	n.a.	6.91

trations that decrease with distance from the seafloor, which indicates that upward fluxes of methane occur across the sediment–water interface. The low δ^{13}C-CH_4 values of the basin waters (−54 to −61‰; Fig. 2) also indicate that biogenic methane from the sediments is the source of methane to the bottom waters.

At both stations, methane decreases in concentration above the seafloor, while the methane isotopic ratios become enriched. The importance of microbial methane oxidation versus simple mixing in controlling the methane distribution was investigated by calculating the apparent kinetic isotopic fractionation factor (α) for methane loss upward from the concentration maximum immediately above the seafloor. Mean values of 1.0072 and 1.0104 were calculated for Sta. 10 and 15, respectively (Table 4), consistent with microbial aerobic methane oxidation being the dominant cause of the decreasing concentrations and increasing δ^{13}C values above the seafloor (*see* Calculations).

The pore-water chemical profiles for Sta. 10 and 15 are quite different considering they are both silled basins (Fig. 4). Sta. 10 has the largest surface sulfate gradient of all the stations, while that of Sta. 15 is much smaller (Table 3). The surface sulfate gradients of pore water in anoxic sediments have been shown to be related to the sedimentation rate and quality of organic matter (Berner 1978; Paez-Osuna and Osuna-Lopez 1990). The large surface sulfate gradient at Sta. 10 indicates that the sedimentation rate there is likely larger than those of the other stations and/or the organic content of the deposited sediment is more diagenetically reactive; the latter situation is indicated by the low C : N ratio of the surface sediment at this site (Table 3). The steep sulfate gradient at Sta. 10 results in a relatively short zone of sulfate reduction (Table 3). The methane concentrations in the sulfate-reduction zone are also the highest at Sta. 10 and thus drive the strongest flux of methane into the overlying water column, whereas the flux at Sta. 15 is one fifth that of Sta. 10 (Table 3). Of course, the presence of a pore-water methane gradient below the sediment–water interface does not necessarily result in a flux of methane across this boundary, as consumption of methane very close to the interface may be occurring at a scale not resolved with our core-sectioning approach.

It is notable that the surface sulfate gradient and the sediment–water methane flux at Sta. 12 are both high, with a sulfate gradient comparable to that at Sta. 10. Although Sta. 12 is not a silled basin, both it and Sta. 10 are situated outside the Gulf of California, which could be the reason for the similarities in their pore-water chemistry. These stations likely have higher sedimentation rates and/or receive a larger percentage of oceanic detritus than Sta. 15 and the other stations inside the Gulf. Because of offshore upwelling-fueled productivity, the oceanic detritus may be more readily degradable than organic matter derived from within the Gulf, as is seen in Tomales Bay, California (Sansone et al. 1998*a*).

The smaller surface sulfate gradient and deeper zone of sulfate reduction at Sta. 15 may then be the result of its position inside the Gulf of California. The proximity of Sta. 15 to the coast and the terrigenous sediments it receives (Nava-Sanchez et al. 2001) could all decrease the relative amount of reactive organic matter in the sediments at this station. Additionally, lower inputs of reactive organic matter could also mean lower inputs of ''noncompetitive'' substrates for methanogens. This, coupled with a deeper sulfate-reduction zone, may keep methane concentrations at this station lower than those of Sta. 10 and 12.

Shallow silled basin—Sta. 31 and 32—Methane concentrations at Sta. 32 are supersaturated throughout the water column, with levels as high as 78 nmol L^{-1} within 10 m of the 450-m–deep seafloor. These concentrations decrease with increasing distance from the sediments but still remain above 20 nmol L^{-1} at 150 m in depth before dropping to 4–5 nmol L^{-1} in the upper 75 m.

Sta. 31 is situated less than 10 km from Sta. 32 and is in the same silled basin, so the pore-water chemistry of the two sites is probably very similar. The surface sulfate gradient at Sta. 31 is not very steep, but the methane flux from the sediments is comparable to that of the open-margin sites Sta. 21 and 26. This indicates that the sulfate is depleted within 400 cm of the sediment–water interface. Although Sta. 31 is technically outside the main Gulf area, it exhibits pore-water chemistry that is more consistent with the Gulf sites than those of offshore Sta. 10 or 12, which appear to have a larger oceanic influence.

If the sole source of methane to the water column at Sta. 32 was methane diffusing/mixing upward from the sediments, then the methane concentrations should decrease and the δ^{13}C-CH_4 values should become enriched with distance from the sediment source (Valentine et al. 2001). This would occur as a result of mixing with low concentrations of isotopically heavy background methane, concurrent with microbial methane oxidation (*see* below). However, the methane concentrations at 250 m fall to half the value of those overlying the sediments, yet the δ^{13}C-CH_4 value is similar to that of the near-bottom water. This indicates that in situ methanogenesis, producing isotopically light methane, may be occurring in the anoxic waters of the basin.

The methane above 250 m decreases in concentration and the isotopic ratios become enriched. However, the δ^{13}C-CH_4 value at 75 m is very high (−22.5‰) compared to values at similar depths at Sta. 10 and 15. The relatively elevated oxygen concentrations at this depth (~4 μmol L^{-1}, Fig. 2) probably result in enhanced microbial methane oxidation and

Table 4. Apparent biological kinetic isotopic fractionation factors (α) calculated using Eqn. (6), along with the depths over which α was calculated.

Station	Depth (m) Initial	Residual	α
10	502	400	1.0071
	520	400	1.0072
15	383	302	1.0103
	352	302	1.0104
24	594	545	1.0108
	594	494	1.0160
30	341	266	1.0120
32	250	149	1.0135
	250	75	1.0061
	149	95	1.0031
			Max = 1.0160
			Min = 1.0031
			Mean = 1.0100
			2.d. = 0.0038

are the likely cause of the low methane concentrations and enriched isotopic ratios found here. To test this hypothesis, α was again calculated for methane loss up through the water column (Table 4). As with Sta. 10 and 15, the α values are consistent with microbial methane oxidation as the cause of the decreasing concentrations and increasing $\delta^{13}C$ values.

Unsilled (open) basin—Sta. 16—Sta. 16 is a 400-m–deep, open basin at the eastern edge of La Paz Bay, with the Sta. 15 basin on its west side and an opening to the Gulf of California to the northeast (Nava-Sanchez et al. 2001). Methane concentrations stay supersaturated with respect to the atmosphere throughout the water column. Methane concentrations are lowest in the deep waters, indicating that the local sediments are not a large source of methane to the water column. This is interesting because, unlike most of the open-margin stations, sediments at Sta. 16 are in the core of the oxygen minimum zone, suggesting that elevated oxygen concentrations are not the reason bottom-water methane concentrations are low here. The small size of the basin (<8% the area of the Sta. 15 basin), coupled with the fact that the Sta. 15 basin traps the majority of terrigenous input (Nava-Sanchez et al. 2001), may cause low sedimentation rates in the basin and, as a result, a low sediment–water methane flux. However, the pore-water methane concentrations and sediment–water flux at Sta. 16 are not known since there was no core analyzed at this site.

Open margin with oxic bottom water—Sta. 14, 19, 21, 24, 26, and 28—Methane concentrations at Sta. 14 and 19 decrease to undersaturated values below the subsurface methane maximum, whereas at Sta. 24 and 28, the concentrations stay at about saturation level (Fig. 3). The seawater density and light transmission profiles at, above, and below these depths show little variability (Graham 2003), indicating that in situ production due to suspended particles is not the cause of these local maxima. The $\delta^{13}C$-CH_4 value of the local maximum at 590 m at Sta. 24 is isotopically depleted (−52.5‰), with values increasing both above and below this depth, a result that is again consistent with microbial methane oxidation being the control (Table 4). Advection of methane-rich pore water from another site to Sta. 24, with little microbial methane oxidation occurring during the advection, could be the source of the mid-depth local maximum. All of these sites have low methane concentrations in the deep waters overlying the sediments, indicating that the sediments are not a significant source of methane to the water column. The pore-water chemistry profiles of the open-margin sites show a high degree of variability between stations. Sta. 21 has a very low surface sulfate gradient, and sulfate concentrations never reach 3 mmol L^{-1} within the depths sampled (Table 3). As a result, methane concentrations throughout the core remain low (<70 μmol L^{-1}), and the flux from the sediment to the water is small. The sedimentation rates at this site are presumably very low and/or the organic matter supplied to the sediments is relatively unreactive; the relatively high C : N ratio of the sediment (Table 3) supports the latter possibility.

The reason the sediments at these open-margin stations do not appear to be large sources of methane to the water column may be a result of the oxygen minimum zone. The core of this zone along the western Mexican margin is situated between 400 and 800 m in water depth, below which the oxygen concentrations begin to slowly increase again (Hartnett et al. 1998; Figs. 2, 3). The sediments of these open-margin stations are situated at 990–2,120 m in depth, resulting in somewhat elevated oxygen concentrations in the waters overlying the sediments (2–25 μmol L^{-1}). These oxygen concentrations may be large enough to support microbial methane oxidation rates higher than those at Sta. 30 and 32, situated in the oxygen minimum zone. These higher rates could effectively keep methane concentrations in the bottom waters low, even though large methane fluxes from the sediments may be present.

Open margin with anoxic bottom water—Sta. 12, 29, and 30—Methane concentrations at Sta. 30 are supersaturated throughout the water column. However, the concentration in the bottom water overlying the sediments is slightly elevated (8 nmol L^{-1}), but is lower than most of the rest the water column, indicating that diffusion from the sediments is not a primary source of methane to the water column. A mid-depth maximum of 28 nmol L^{-1} is found at 340 m and is associated with an isotopically depleted $\delta^{13}C$-CH_4 value of −55‰. Unlike Sta. 24, where $\delta^{13}C$-CH_4 values increase dramatically (up to −32‰) above and below the mid-depth maximum, similar samples at Sta. 30 remain relatively depleted (−45 to −50‰).

The elevated concentration and the isotopically relatively depleted $\delta^{13}C$-CH_4 value at the methane maximum at 340 m indicate that methane below 200 m could either be produced in situ or could be advected from a nearby source with little microbial oxidation occurring. However, α values calculated for samples above and below the 340-m maximum (Table 4) are again consistent with microbial oxidation as the control on the observed variation, implying a significant role for in situ methane production.

A comparison of the sediment profiles for Sta. 12 and 29

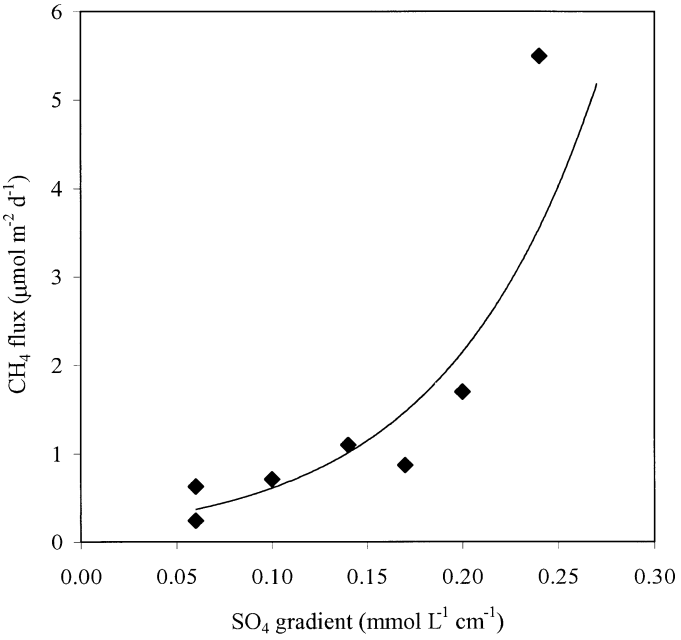

Fig. 6. Calculated diffusive methane flux versus surface sulfate gradient for CALMEX core stations (data from Table 3). The regression line is $y = 0.174e^{12.6x}$ ($r^2 = 0.82$).

again demonstrates the higher reactivity of the offshore environment west of Baja California (Sta. 12) versus that offshore of the Mexican mainland (Sta. 29). The similar surface-sediment C : N ratios of these two sites argues that this difference may be more attributable to differences in sedimentation rate than to differences in the character of the sediment organic matter.

Methane cycling along the western Mexican margin—There is large variation in the sediment pore-water chemistry between sites. The highest surface sulfate gradients, largest methane fluxes, and shallowest sulfate-depleted zones are found on the Pacific side of Baja California, indicating that oceanic processes (e.g., higher sedimentation rates, more labile organic matter) may play a role at these sites. Inside the Gulf of California, the sulfate gradients and methane fluxes are much lower, and they vary greatly between stations. Advection of phytoplankton away from the coast, the gradient in phytoplankton communities with latitude in the Gulf, and local influences from rivers (Santamaria-del-Angel et al. 1994) could affect the quality and quantity of organic matter reaching the seafloor, which probably results in the high variability of pore-water chemistry observed between stations.

One interesting observation from the chemical data presented in Table 3 is the existence of a positive relationship between the calculated diffusive methane flux and the measured surface sulfate gradient (Fig. 6). If this relationship is seen in other margin settings, the ease of measuring sulfate gradients may, in the future, make it a useful proxy for methane flux measurements.

The silled basins have high methane concentrations in their bottom waters as a result of release from methane-rich pore water in the sediment. The low oxygen concentrations and reduced circulation (longer water residence time) in the basins result in the build-up of this methane below the sills of the basins. However, methane concentrations at sill depth were low in the basins we studied, indicating that basins may not release large amounts of methane to margin waters.

The open-margin stations with water depths of around 1,000 m also do not appear to supply elevated methane concentrations to the ETNP, in this case because of the low subsurface methane concentrations present throughout the water column. The sediments present at these stations are below the core of the oxygen minimum zone; significant oxygen concentrations, and resulting aerobic methane oxidation, in the water overlying these sediments may limit the amount of methane reaching the water column.

The primary margin sites supplying methane to the ETNP appear to be those with seafloors that intersect the oxygen minimum zone, such as Sta. 30. The low oxygen concentrations overlying these sediments likely result in lower microbial methane oxidation rates, allowing enhanced methane concentrations to develop in the water column. While Sta. 30 does not have a large input of methane from the sediments, methane concentrations are elevated throughout the water column, with evidence for either rapid advection from a methane-rich sediment source or in situ production.

If advection of methane from sediments in the oxygen minimum zone is occurring, it would be expected that a large methane signal would be generally present between 200 and 600 m at the open-margin hydrocast sites. Instead, only small signals are observed at Sta. 24 and 28, with no observable signal at Sta. 14 and 19. This lack of methane in the oxygen minimum zone at these sites may in part be explained by the currents of the Gulf of California. Collins et al. (1997) performed one of the few observational current studies in the southern Gulf of California. Using an acoustically tracked dropsonde (deployed near Sta. 24), they studied the currents across the entrance to the Gulf, starting at the tip of Baja California and moving northeast to mainland Mexico. Throughout most of the year, the currents along the eastern coast of the Gulf appear to flow to the northeast, toward mainland Mexico. In such a case, methane-rich pore waters along the eastern side of the entrance of the Gulf would be advected eastward into shallower waters, away from the deeper open margin. Thus, the lack of a major methane signal in the oxygen minimum zone of the deeper offshore stations does not preclude the possibility of a large flux of methane from nearby, shallower sediments that intersect the oxygen minimum zone.

Finally, an examination of the entire carbon stable isotopic data set shows clearly the effects of microbial oxidation on the methane dynamics of the western Mexican shelf. Specifically, there is a good logarithmic relationship between methane concentration and the methane stable-carbon isotopic ratio for CALMEX hydrocast stations, both basin and open margin (Fig. 7). Moreover, the entire hydrocast stable isotopic data set can be modeled as an initial methane concentration of 79 nmol L^{-1} (the highest hydrocast concentration) that is microbially oxidized with an kinetic isotope fractionation factor (α) of 1.0650 (Fig. 7). This α value is within the range expected for microbially mediated oxidation (*see* Calculations) and is consistent with values obtained at individual stations (Table 4).

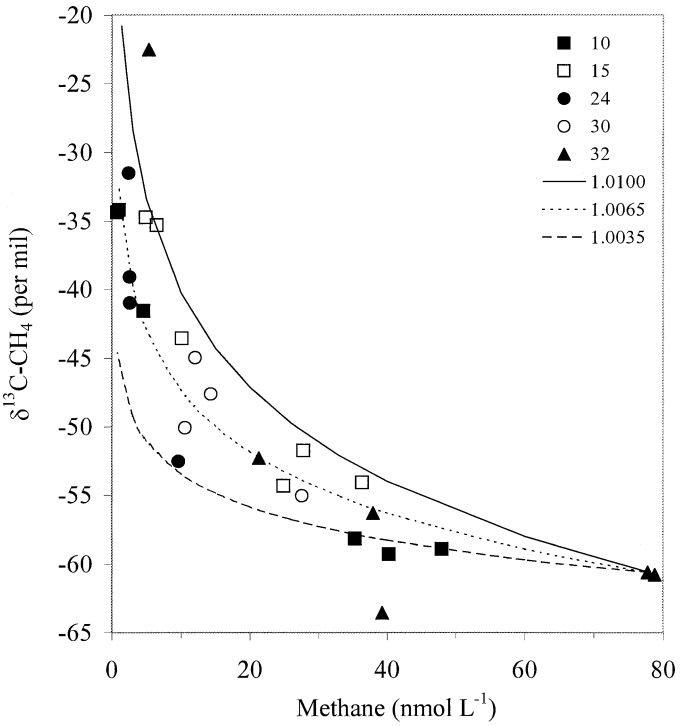

Fig. 7. Methane concentration versus methane stable-carbon isotopic ratio for CALMEX hydrocast stations. Theoretical isotopic fractionation curves are also shown for α values of 0.0035, 1.0065, and 1.0100 (computed using Eq. 14 of Coleman and Risatti [1981]). The regression (not shown) for all of the hydrocast data is $y = -7.393\ln(x) - 29.14$ ($r^2 = 0.7555$).

The Mexican margin as a source of ETNP methane—The water-column methane profiles from the CALMEX cruise show that the large pool of dissolved methane between 200 and 600 m in the ETNP is not present everywhere along the western Mexican margin. Burke et al. (1983) suggested that the low oxygen concentrations in the ETNP, in conjunction with in situ methane production, resulted in the elevated methane concentrations there, similar to the situation reported by Jayakumar et al. (2001) for the Arabian Sea. Although there is evidence for net in situ methanogenesis in the water column at the CALMEX sites (i.e., elevated methane concentrations and isotopically depleted $\delta^{13}C$ values), this production is limited to the upper 350 m.

Two plausible sources for the 200–600-m–deep ETNP methane pool are the sediments (Sansone et al. 2001) and methane hydrates or seeps along the western Mexican margin. Exploration of methane hydrates and seeps was outside the scope of this research, which focused on the sediments of the margin. However, hydrates and seeps should not be overlooked, as they could potentially be a significant source of methane to the water column, as has been reported for other North American margins (e.g., Carson et al. 1990).

Diffusive methane fluxes from the sediment, as estimated from sediment methane gradients, were 0.24–5.5 μmol m^{-2} d^{-1}, with the highest fluxes observed on the Pacific margin of Baja California at both basin and open-margin sites. These high rates occur despite the lack of significant terrestrial input to these sediments, reflecting the importance of upwelling-induced productivity. We observed an inverse relationship between methane concentration and $\delta^{13}C$-CH_4 value in the water column, consistent with biological aerobic oxidation of methane being released from the sediment; an apparent kinetic isotopic fractionation factor of 1.0100 $\pm$ 0.0038 was calculated for this process, consistent with the results of previous studies (*see* Calculations). Isotopic heavy methane resulting from this oxidation may be the source of large pools of heavy methane previously observed offshore in the ETNP.

Stations with sediments below the oxygen minimum zone showed little methane accumulation in subsurface water, indicating little or no net input of methane from the sediments. In contrast, Sta. 32, with sediments located in an anoxic basin, had highly elevated methane concentrations in the water column as a result of fluxes from the sediments. However, the methane flux from the sediments at nearby Sta. 31 is low (Table 3). A similar situation is seen at Sta. 30, the shallow open-margin site: elevated subsurface water-column methane concentrations despite very low sediment release rates.

This result indicates that the factor controlling the methane concentration of the water column along the western Mexican margin, and ultimately the ETNP, is not the magnitude of the flux of methane from the sediments, but whether the surface of these sediments are located in the core of the oxygen minimum zone. Low sediment–water fluxes of methane can cause high methane concentrations in the overlying waters as long as these fluxes are occurring into waters that are severely oxygen depleted, presumably reflecting the requirement of molecular oxygen for aerobic methane oxidation (e.g., Sansone and Martens 1978). Thus, methane could then be advected away from its source with relatively little microbial oxidation occurring as long as the methane stayed within the oxygen minimum zone.

The severely depleted oxygen concentrations of the ETNP extend south of Sta. 32 along the western Mexican margin (Fig. 1); sediments along the margin that intersect these anoxic waters are likely sites of elevated subsurface methane concentrations. The advection of methane-rich bottom waters overlying these sediments in the oxygen minimum zone is likely to be a significant source of methane to the ETNP.

The relatively shallow depth of the anoxic core of the oxygen minimum zone along the western Mexican margin is probably significant, given that it results in anoxia-impacted sediments that are closer to the shoreline than would otherwise be the case. Such sediments would presumably be more productive than those deposited under a deeper oxygen minimum zone. This, perhaps, makes the anoxic–bottom-water hypothesis presented above more important along the western Mexican margin than in coastal environments without significant upwelling or terrestrial organic inputs.

References

BANGE, H. W., U. H. BARTELL, S. RAPSOMANIKIS, AND M. O. ANDREAE. 1994. Methane in the Baltic and North Seas and a reassessment of the marine emissions of methane. Global Biogeochem. Cycles **8:** 465–480.

BARBER, T., R. BURKE, JR., AND W. SACKETT. 1988. Diffusive flux

of methane from warm wetlands. Global Biogeochem. Cycles **2:** 411–425.

BARNES, R., AND E. GOLDBERG. 1976. Methane production and consumption in anoxic marine sediments. Geology **4:** 297–300.

BERNER, R. 1971. Principals of chemical sedimentology, 1st ed. McGraw-Hill.

———. 1978. Sulfate reduction and the rate of deposition of marine sediments. Earth Plant. Sci. Lett. **37:** 492–498.

BREAS, O., C. GUILLOU, F. RENIERO, AND E. WADA. 2001. The global methane cycle: Isotopes and mixing ratios, sources and sinks. Isotopes Environ. Health Stud. **37:** 257–379.

BROOKS, J. 1979. Deep methane maxima in the Northwest Caribbean Sea: Possible seepage along the Jamaica ridge. Science **206:** 1069–1071.

———, D. REID, AND B. BERNARD. 1981. Methane in the upper water column of the northwestern Gulf of Mexico. J. Geophys. Res. **86:** 11029–11040.

BURKE, R., JR., D. REID, J. BROOKS, AND D. LAVOIE. 1983. Upper water column methane geochemistry in the eastern tropical North Pacific. Limnol. Oceanogr. **28:** 19–32.

CARSON, B., E. SUESS, AND J. S. STRASSNER. 1990. Fluid flow and mass flux determinations at vent sites on the Cascadia margin accetionary prism. J. Geophys. Res. **95B:** 8891–8897.

CICERONE, R., AND R. OREMLAND. 1988. Biogeochemical aspects of atmospheric methane. Global Biogeochem. Cycles **2:** 299–327.

CLINE, J., AND F. RICHARDS. 1972. Oxygen deficient conditions and nitrate reduction in the eastern tropical North Pacific Ocean. Limnol. Oceanogr. **17:** 885–900.

COLEMAN, D., AND J. RISATTI. 1981. Fractionation of carbon and hydrogen isotopes by methane-oxidizing bacteria. Geochim. Cosmochim. Acta **45:** 1033–1037.

COLLINS, C., N. GARFIELD, A. MASCARENHAS, JR., M. SPEARMAN, AND T. RAGO. 1997. Ocean currents across the entrance to the Gulf of California. J. Geophys. Res. **102:** 20, 927, 936.

CONRAD, R., AND W. SEILER. 1988. Methane and hydrogen in seawater (Atlantic Ocean). Deep-Sea Res. **35:** 1903–1917.

COWEN, J., X. WEN, AND B. POPP. 2002. Methane in aging hydrothermal plumes. Geochim. Cosmochim. Acta **66:** 3563–3571.

CRAIG, H. 1957. Isotopic standards for carbon and oxygen and correction factors for mass spectometric analyses of carbon dioxide. Geochim. Cosmochim. Acta **12:** 133–149.

DE ANGELIS, M., AND C. LEE. 1994. Methane production during zooplankton grazing on marine phytoplankton. Limnol. Oceanogr. **39:** 1298–1308.

———, ———, E. OLSON, AND J. BAROSS. 1993. Methane oxidation in deep-sea hydrothermal plumes of the Endeavour Segment of the Juan de Fuca Ridge. Deep-Sea Res. **40:** 1169–1186.

———, AND M. LILLEY. 1987. Methane in surface waters of Oregon estuaries and rivers. Limnol. Oceanogr. **32:** 716–722.

DEUSER, W. 1975. Reducing environments, p. 1–37. *In* J. Riley and G. Skirrow [eds.], Chemical oceanography, v. 3, 2nd ed. Academic.

GHARIB, J. 2000. Methane in hydrothermal plumes along the East Pacific Rise, 28–32°S. M.S. thesis. Univ. of Hawaii.

GRAHAM, A. W. 2003 Methane along the western Mexican margin. M.S. thesis. Univ. of Hawaii.

GROSSMAN, E., L. CIFUENTES, AND I. COZZARELLI. 2002. Anaerobic methane oxidation in a landfill-leachate plume. Environ. Sci. Technol. **36:** 2436–2442.

HARTNETT, H., R. KEIL, J. HEDGES, AND A. DEVOL. 1998. Influence of oxygen exposure time on organic carbon preservation in continental margin sediments. Nature **391:** 572–574.

HOLMES, M., F. J. SANSONE, T. RUST, AND B. POPP. 2000. Methane production, consumption, and air–sea exchange in the open ocean: An evaluation based on carbon isotopic ratios. Global Biogeochem. Cycles **14:** 1–10.

INTERGOVERNMENTAL PANEL ON CLIMATE CHANGE (IPCC). 2001. Climate change 2001: The scientific basis, p. 239–287. *In* J. Houghton, Y. Ding, D. Griggs, and M. Noguer [eds.], Contribution of Working Group I to the Third Assessment Report. Cambridge Univ. Press.

IVERSEN, N., AND B. JORGENSEN. 1985. Anaerobic methane oxidation rates at the sulfate-methane transition in marine sediments from Kattegat and Skagerrak (Denmark). Limnol. Oceanogr. **30:** 944–955.

JAYAKUMAR, D. A., S. W. A. NAQVI, P. V. NARVEKAR, AND M. D. GEORGE. 2001. Methane in coastal and offshore waters of the Arabian Sea. Mar. Chem. **74:** 1–13.

KARL, D., AND B. TILBROOK. 1994. Production and transport of methane in oceanic particulate organic matter. Nature **368:** 732–734.

KELLEY, C. A., AND W. H. JEFFREY. 2002. Dissolved methane concentration profiles and air-sea fluxes from 41°S to 27°N. Global Biogeochem. Cycles **16:** 13-1-13-6 (doi:10.1029/2001GB001809).

LAMONTAGNE, R., J. SWINNERTON, V. LINNENBOM, AND W. SMITH. 1973. Methane concentrations in various marine environments. J. Geophys. Res. **78:** 5317–5324.

MARTENS, C., D. ALBERT, AND M. ALPERIN. 1999. Stable isotope tracing of methane production and oxidation in the gassy sediments of Eckernförde Bay, German Baltic Sea. Am. J. Sci. **299:** 589–610.

———, AND R. BERNER. 1974. Methane production in the interstitial waters of sulfate depleted marine sediments. Science **185:** 1167–1169.

———, AND ———. 1977. Interstitial water chemistry of anoxic Long Island Sound sediments I. Dissolved gases. Limnol. Oceanogr. **22:** 10–25.

———, N. BLAIR, C. GREENS, AND D. DES MARAIS. 1986. Seasonal variations in the stable carbon isotopic signature of biogenic methane in a coastal sediment. Science **233:** 1300–1303.

———, AND J. KLUMP. 1980. Biogeochemical cycling in an organic rich coastal marine basin I. Methane sediment water exchange processes. Geochim. Cosmochim. Acta **44:** 471–490.

MCDUFF, R., AND J. GIESKES. 1976. Calcium and magnesium profiles in DSSP interstitial waters: Diffusion or reaction? Earth Planet. Sci. Lett. **33:** 1–10.

MOTTL, M., F. J. SANSONE, C. WHEAT, J. RESING, E. BAKER, AND J. LUPTON. 1995. Manganese and methane in hydrothermal plumes along the East Pacific Rise, 8°40′ to 11°50′N. Geochim. Cosmoschim. Acta **59:** 4147–4165.

NAVA-SANCHEZ, E., D. GORSLINE, AND A. MOLINA-CRUZ. 2001. The Baja California peninsula borderland: Structural and sedimentological characteristics. Sed. Geol. **144:** 63–82.

OREMLAND, R. 1979. Methanogenic activity in plankton samples and fish intestines: A mechanism for in-situ methanogenesis in oceanic surface waters. Limnol. Oceanogr. **24:** 1136–1141.

——— and B. F. TAYLOR. 1978. Sulfate reduction and methanogenesis in marine sediments. Geochim. Cosmochim. Acta **42:** 209–214.

OUDOT, C., P. JEAN-BAPTISTE, E. FOURRE, C. MORMICHE, M. GUEVEL, J.-F. TERNON, AND P. LE CORRE. 2002. Transatlantic equatorial distribution of nitrous oxide and methane. Deep-Sea Res. I **49:** 1175–1193.

OWENS, N., C. LAW, R. MANTOURA, P. BURKILL, AND C. LLEWELLYN. 1991. Methane flux to the atmosphere from the Arabian Sea. Nature **354:** 293–296.

PAEZ-OSUNA, F., AND J. OSUNA-LOPEZ. 1990. The initial gradient of sulfate in Gulf of California sediments. J. Sed. Petrol. **6:** 912–917.

POPP, B. N., F. J. SANSONE, T. RUST, AND D. MERRITT. 1995. De-

termination of concentration and carbon isotopic composition of dissolved methane in sediments and nearshore waters. Anal. Chem. **67:** 405–411.

REEBURGH, W. 1976. Methane consumption in Cariaco Trench waters and sediments. Earth Planet. Sci. Lett. **28:** 337–344.

———, AND D. HEGGIE. 1977. Microbial methane consumption reactions and their effect on methane distributions in freshwater and marine environments. Limnol. Oceanogr. **22:** 1–9.

REHDER, G., R. W. COLLIER, K. HEESCHEN, P. M. KOSRO, J. BARTH, AND E. SUESS. 2002. Enhanced marine CH_4 emissions to the atmosphere off Oregon caused by coastal upwelling. Global Biogeochem. Cycles **16:** 10.1029/2000GB001391.

SAHORES, J., AND P. WITHERSPOON. 1970. Diffusion of light paraffin hydrocarbons in water from 2 to 80°C, p. 219–230. *In* G. Hobson, and G. Spears [eds.], Advances in organic geochemistry. Pergamon Press.

SANSONE, F. J., M. HOLMES, AND B. N. POPP. 1999. Methane stable isotopic ratios and concentrations as indicators of methane dynamics in estuaries. Global Biogeochem. Cycles **13:** 463–474.

———, AND C. S. MARTENS. 1978. Methane oxidation in Cape Lookout Bight, N.C. Limnol. Oceanogr. **23:** 349–355.

———, B. N. POPP, A. GASC, A. W. GRAHAM, AND T. M. RUST. 2001. Highly elevated methane in the eastern tropical North Pacific and associated isotopically enriched fluxes to the atmosphere. Geophys. Res. Lett. **28:** 4567–4570.

———, ———, S. B. JOYE, AND R. M. CHAMBERS. 1998*a*. Carbon cycling and isotopic geochemistry in sediments along a marine-terrestrial organic matter gradient: Tomales Bay, Calif. Eos (suppl.) **79:** OS94 (abstract).

———, ———, AND T. M. RUST. 1997. Stable carbon isotopic analysis of low-level methane in water and gas. Anal. Chem. **69:** 40–44.

———, T. M. RUST, AND S. V SMITH. 1998*b*. Methane distribution and cycling in Tomales Bay, California. Estuaries **21:** 66–77.

SANTAMARIA-DEL-ANGEL, E., S. ALVAREZ-BORREGO, AND F. MULLER-KARGER. 1994. Gulf of California biogeographic regions based on coastal zone color scanner imagery. J. Geophys. Res. **99:** 7411–7421.

SCHOELL, M. 1980. The hydrogen and carbon isotopic composition of methane from natural gases of various origins. Geochim. Cosmochim. Acta **44:** 649–661.

SCRANTON, M., AND P. BREWER. 1977. Occurrence of methane in the near-surface waters of the western subtropical North-Atlantic. Deep-Sea Res. **24:** 127–138.

———, AND J. FARRINGTON. 1977. Methane production in the waters off Walvis Bay. J. Geophys. Res. **83:** 4947–4953.

STEELE, L. P., P. B. KRUMMEL, AND R. L. LANGENFELDS. 2002. Atmospheric CH_4 concentrations from sites in the CSIRO Atmospheric Research GASLAB air sampling network (October 2002 version). *In* Trends: A compendium of data on global change, Carbon Dioxide Information Analysis Center, Oak Ridge National Laboratory, U.S. Department of Energy, Oak Ridge, TN.

SUESS, E., AND OTHERS. 1999. Gas hydrate destabilization: Enhanced dewatering, benthic material turnover and large methane plumes at the Cascadia convergent margin. Earth Planet. Sci. Lett. **170:** 1–15.

VALENTINE, D. L., D. BLANTON, W. S. REEBURGH, AND M. KASTNER. 2001. Water column methane oxidation adjacent to an area of active hydrate dissociation, Eel River Basin. Geochim. Cosmochim. Acta **65:** 2633–2640.

———, AND W. S. REEBURGH. 2000. New perspectives on anaerobic methane oxidation (mini review). Environ. Microbiol. **2:** 477–484.

WARFORD, A., D. KOSIUR, AND P. DOOSE. 1979. Methane production in Santa Barbara Basin sediments. Geomicrobiol. J. **1:** 117–137.

WELHAN, J. 1988. Origins of methane in hydrothermal systems. Chem. Geol. **71:** 183–198.

WHITICAR, M. 1996. Isotope tracking of microbial methane formation and oxidation. Mitt. Internat. Verein. Limnol. **25:** 39–54.

———, E. FABER, AND M. SCHOELL. 1986. Biogenic methane formation in marine and freshwater environments: CO_2 reduction vs. acetate fermentation—isotope evidence. Geochim. Cosmochim. Acta **50:** 693–709.

YAMAMOTO, S., J. ALCAUSKAS, AND T. CROZIER. 1976. Solubility of methane in distilled water and seawater. J. Chem. Eng. Data **21:** 78–80.

Received: 6 June 2003
Accepted: 30 March 2004
Amended: 15 June 2004